Received: 7 August 2019 | Revised: 3 December 2019 | Accepted: 16 December 2019
DOI: 10.1002/aoc.5646

FULL PAPER

Applied Organometallic Chemistry WILEY

Reduced graphene oxide supported copper oxide nanocomposites: An efficient heterogeneous and reusable catalyst for the synthesis of ynones, 1,3-diynes and 1,5-benzodiazepines in one-pot under sustainable reaction conditions

Rajib Sarkar | **Ajay Gupta** | **Ramen Jamatia** | **Amarta Kumar Pal**

Department of Chemistry, Centre for Advanced Studies, North-Eastern Hill University, Shillong, 793022, India

Correspondence
Amarta Kumar Pal, Department of Chemistry, Centre for Advanced Studies, North-Eastern Hill University, Shillong, 793022, India.
Email: amartya_pal22@yahoo.com; akpal@nehu.ac.in

Funding information
Science and Engineering Research Board, Grant/Award Number: EMR/2016/005089 dated 30.6.2017; North-Eastern Hill University; University Grant Commission (UGC)

A greener and efficient method for the synthesis of ynones and 1,3-diynes using copper oxide nanoparticles (CuONPs) doped reduced graphene oxide (CuO@rGO) catalyst under palladium, ligand and solvent free conditions have been developed. The catalyst was subsequently utilized for the synthesis of biologically active 1,5-benzodiazepines in one pot via sequential addition of acyl chlorides, terminal alkynes and o-phenylenediamines. The methodology initially involves in situ formation of ynones which react with o-phenylenediamines in presence of ethanol to afford a wide variety of benzodiazepines. Mild reaction conditions, good to an excellent yield of the products, cheap and recyclable catalyst make this methodology environmentally benign and sustainable.

KEYWORDS

1,5-benzodiazepines, cross-coupling, one-pot synthesis, CuO@rGO nanoparticles, homo-coupling, ynones

1 | INTRODUCTION

Synthesis of *α*,*β*-acetylenic carbonyl derivatives (ynones) and 1,3-diynes has been extensively studied over the years due to their wide application in the synthesis of natural products, pharmaceutical and heterocyclic compounds.[1, 2] Several classical methods for their synthesis are cited in the literature.[3–12] In recent years, palladium-catalyzed Sonogashira type of cross-coupling reaction among acyl chloride and terminal alkynes has received much attention because of its easy accessibility to such ynones. C. Zhang and co-workers reported the palladium catalyzed carbonylative reaction for the development of ynones.[13] However, the disadvantage of this methodology is the use of toxic CO gas in the reaction. M. Cui and co-workers reported Pd $(PPh_3)_2Cl_2$ catalyzed cross-coupling of amide derivatives with terminal alkynes to yield ynones, but the reaction proceeds in the presence of solvent like THF and requires a much longer time to complete.[14] In fact, uses of Cu and Pd complexes in these reactions are well reported.[15, 16] However, most

https://doi.org/10.1002/aoc.5646

of these catalysts are homogeneous and unrecyclable. Various other catalysts containing copper and palladium have also been reported in the literature for the coupling of acyl chlorides and terminal alkynes. But the use of such costly palladium and CuI as co-catalyst, limits their application for such transformations.[17, 18] On the other hand, bimetallic catalysts such as Pd/Cu, Ni/Cu and other heterogeneous Cu catalysts have been used for the synthesis of 1,3-diynes.[19, 20] Biswas and group reported the coupling of alkynes using copper oxide supported on manganese oxide in the presence of toluene at a higher temperature of 105 °C.[21]

Recently, metal nano-catalysts because of their higher catalytic activity have been employed for various organic transformation reactions such as selective oxidation,[22] hydrogenation,[23] C-C coupling[24] etc. However, due to higher surface energy, nanoparticles tend to agglomerate themselves which in-turn reduces catalytic activity.[25] In this regard, heterogeneous solid supported with a large surface area, which inhibits nanoparticle agglomeration and thereby increasing its catalytic activity will be desirable. Graphene oxide or reduced graphene oxide nanosheets with a very large surface area containing various oxygenated functional groups tend to anchor metal nanoparticles on its surface effectively.[26] Therefore, we wish to develop reduced graphene oxide supported copper oxide nanocomposites as a reusable catalyst for the aforementioned synthesis. Further ynones are versatile bifunctional synthons for the synthesis of pharmacologically and biologically active heterocycles like

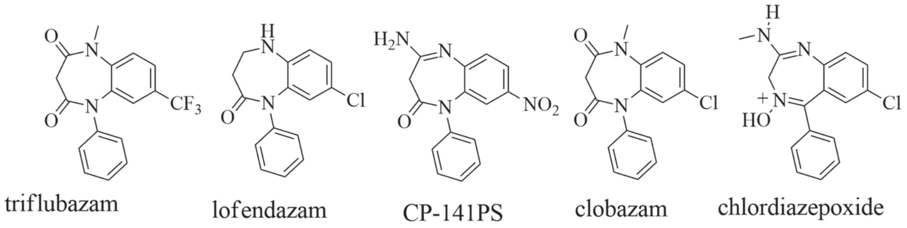

FIGURE 1 Some biologically and pharmacologically active benzodiazepine compounds

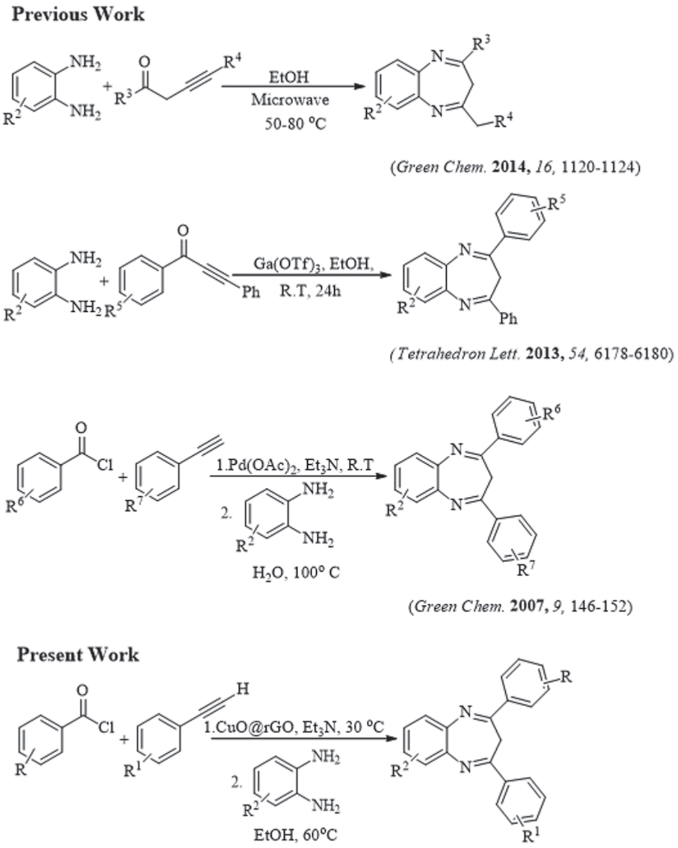

SCHEME 1 Synthesis of 1.5-benzodiazepines

benzodiazepines. These benzodiazepines have immense biological activities such as anti-inflammatory, anti-depressive, anticonvulsant, analgesic, hypnotic and sedation.[27] Some of the biologically and pharmacologically active benzodiazepines e.g. triflubazam, lofendazam, CP-141PS, clobazam, chlordiazepoxide are shown in Figure 1. Agnes Solan et al and S.-G. Huang group demonstrated the use of ynones derivatives for the synthesis of benzodiazepines using microwave irradiation at 50–80 °C[28] or expensive and moisture sensitive Ga $(OTf)_3$ as a catalyst[29] respectively. K. V. Srinivasan and co-workers reported[30] the one-pot synthesis of benzodiazepines utilizing Pd $(OAc)_2$ as a catalyst at 100 °C (Scheme 1). However, this methodology suffers the drawback of the use of costly and non-recyclable catalyst. Therefore, we decided to develop a protocol for the synthesis of ynones, 1,3-diynes and benzodiazepines (Scheme 1, present work) which is cheap, environmental friendly and sustainable. Therefore, we herein report CuO@rGO catalyzed synthesis of said compounds under palladium, ligand and solvent free reaction conditions.

2 | RESULT AND DISCUSSIONS

Graphite Oxide (GO) and CuO@rGO were prepared by the reported procedure (Scheme 2).[31, 32] CuO@rGO was synthesized by the mixing of GO (30 mg) with 200 ml aqueous solution of $CuCl_2$ (9% w/v), and the mixture was then ultrasonicated for 1 hr. To the resulting suspension, $NaBH_4$ (10 ml, 1%) was added slowly which was then heated at 100 °C for 24 hr, and cooled to 50 °C, separated by centrifugation, washed with DI water (3 × 10 ml), methanol (3 × 10 ml) and finally diethyl ether (3 × 10 ml). The resulting CuO@rGO nanocomposites were dried at 100 °C under vacuum.[32] After synthesis, the catalyst was characterized by transmission electron microscopy (TEM), electron dispersive X-ray spectroscopy (EDX), powder XRD, FT-IR, inductively coupled plasma atomic emission spectroscopy (ICP-AES) and Barrett–Joyner–Halenda (BET) analysis.

Powder XRD analysis was used to investigate the formation of GO and CuO@rGO nanocomposites. It is clearly observed that the GO (Figure 2a) has diffraction peaks at 9.33° and 42.20° due to distinctive [001]

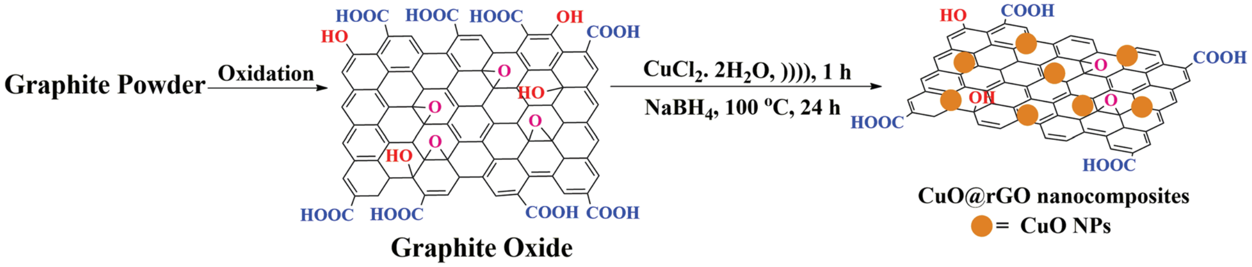

SCHEME 2 Synthesis of CuO@rGO nanocomposites

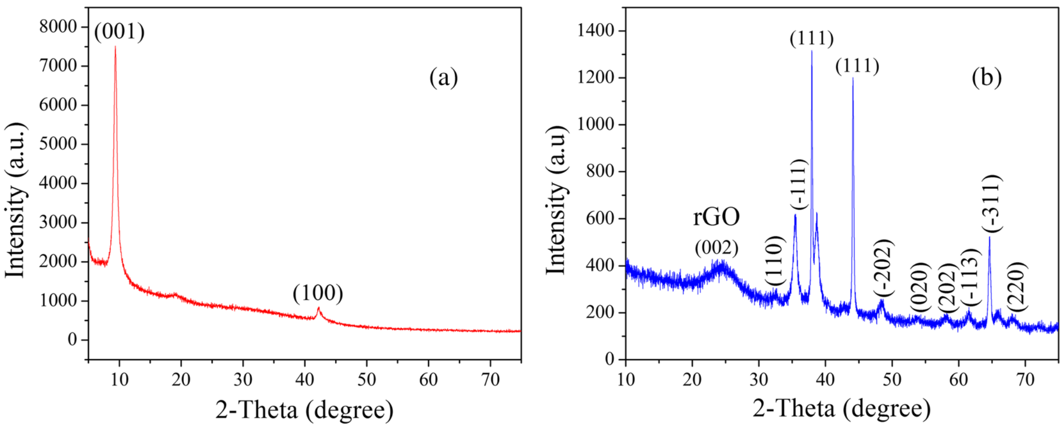

FIGURE 2 PXRD pattern of (a) GO and (b) CuO@rGO nanocomposites

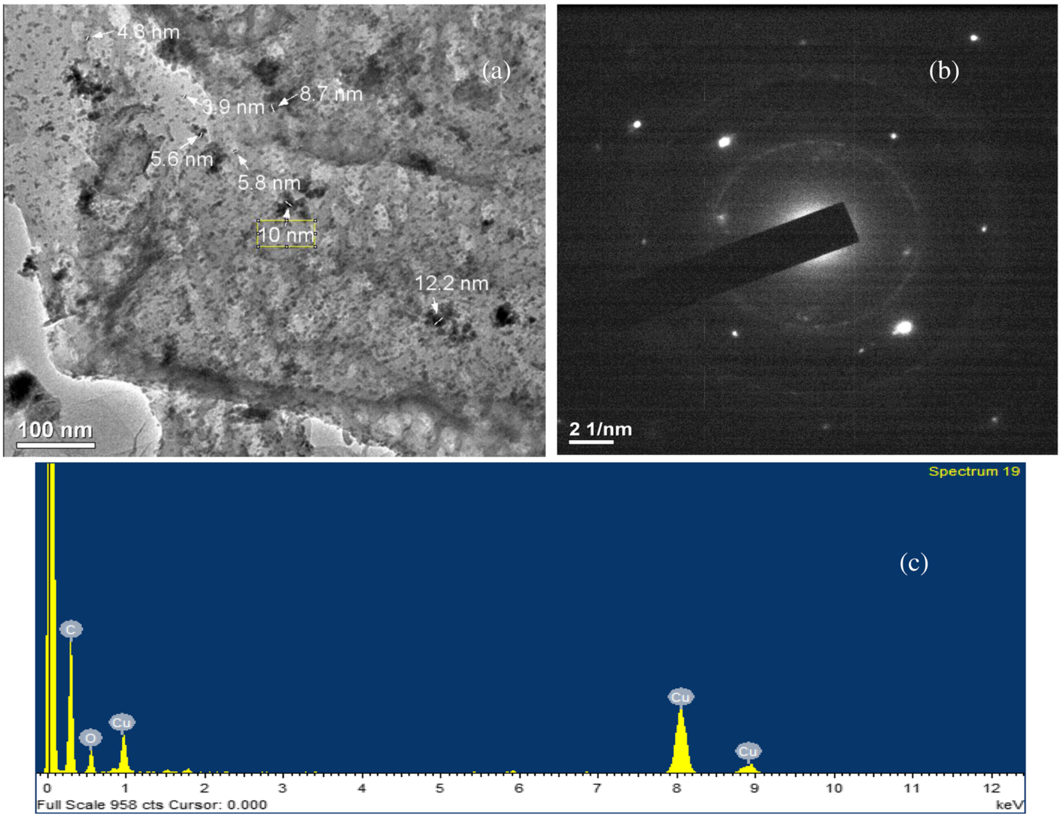

FIGURE 3 TEM image of CuO@rGO nanocomposites at 100 nm (a), SAED pattern (b) and EDX spectrum (c) of CuO@rGO nanocomposites

and [100] planes which display the oxidation of graphite to graphite oxide (GO).[33] The XRD pattern of CuO@rGO nanocomposites (Figure 2b) exhibits new diffraction peak at $2\theta = 24.4^{\circ}$ (002) which indicates a high degree of reduction of GO to rGO during the

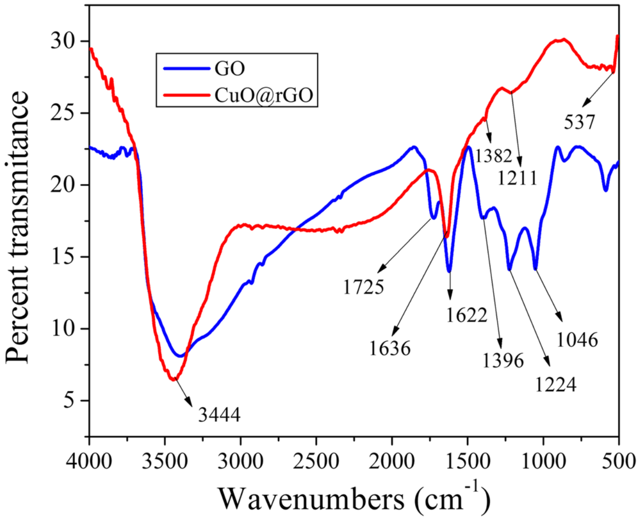

FIGURE 4 Comparative FT-IR spectra of GO and CuO@rGO nanocomposites

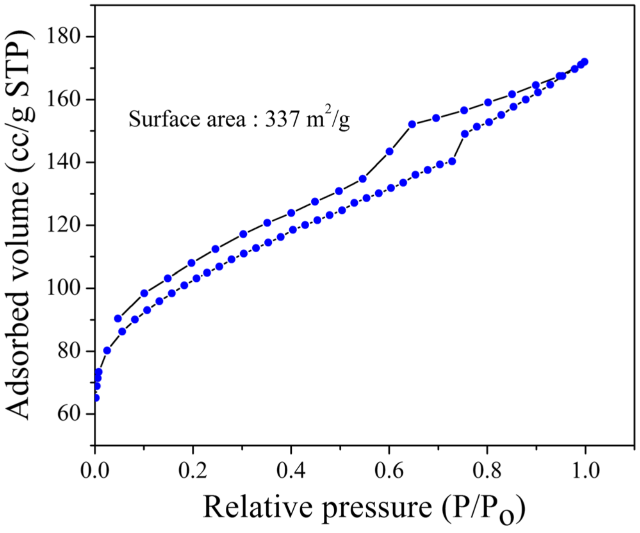

FIGURE 5 N_2-sorption isotherm CuO@rGO nanocomposites

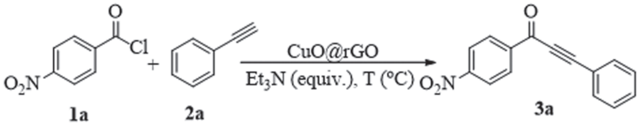

SCHEME 3 Model reaction for CuO@rGO catalyzed cross coupling of acyl chloride and terminal alkyne

TABLE 1 Screening of Reaction Conditions

Entry	Catalyst (mol %)	Base (equiv.)	Solvent	Temp.(°C)	Product	Yield%[aa]
1	Free	Free	Free	RT	3a	ND
2	Free	Free	Free	80	3a	ND
3	CuO@rGO (0.8)	Free	Free	RT	3a	ND
4	CuO@rGO (0.8)	Free	Free	80	3a	ND
5	Free	Et_3N(5)	Free	80	3a	ND
6	CuO@rGO (0.8)	Et_3N(5)	Free	60	3a	96
7	CuO@rGO (0.8)	Et_3N(4)	Free	60	3a	96
8	CuO@rGO (0.8)	Et_3N(3)	Free	60	3a	96
9	**CuO@rGO (0.8)**	**Et_3N(3)**	**Free**	**30**	**3a**	**96**
10	CuO@rGO (0.8)	Et_3N(2)	Free	30	3a	89
11	CuO@rGO (1.2)	Et_3N(3)	Free	30	3a	96
12	Pd $(OAc)_2$ (0.8)	Et_3N(3)	Free	30	3a	92
13	$PdCl_2$ (0.8)	Et_3N(3)	Free	30	3a	90
14	Pd/C (0.8)	Et_3N(3)	Free	30	3a	93
15	Pd $(PPh_3)_2Cl_2$(0.8)	Et_3N(3)	Free	30	3a	90
16	CuO@rGO (0.8)	K_2CO_3(3)	Free	30	3a	ND
17	CuO@rGO (0.8)	Cs_2CO_3(3)	Free	30	3a	ND
18	CuO@rGO (0.8)	BZA(3)	Free	30	3a	ND
19	CuO@rGO (0.8)	Pyridine (3)	Free	30	3a	ND
20	CuO@rGO (0.8)	DIPEA(3)	Free	30	3a	48
21	CuO@rGO (0.8)	Et_3N(3)	Dichloromethane	30	3a	52
22	CuO@rGO (0.8)	Et_3N(3)	Toluene	30	3a	83
23	CuO@rGO (0.8)	Et_3N(3)	Ethanol	30	3a	87
24	CuO@rGO (0.8)	Et_3N(3)	Acetonitrile	30	3a	16
25	CuO@rGO (0.8)	Et_3N(3)	Dimethylformamide	30	3a	12

Reaction conditions: Reactions were carried out using **1a** (1.2 mmol), **2a** (1 mmol) in presence of Et_3N (3 equiv.) and 0.8 mol % of catalyst, CuO@rGO.

[a] Yields of isolated pure products.

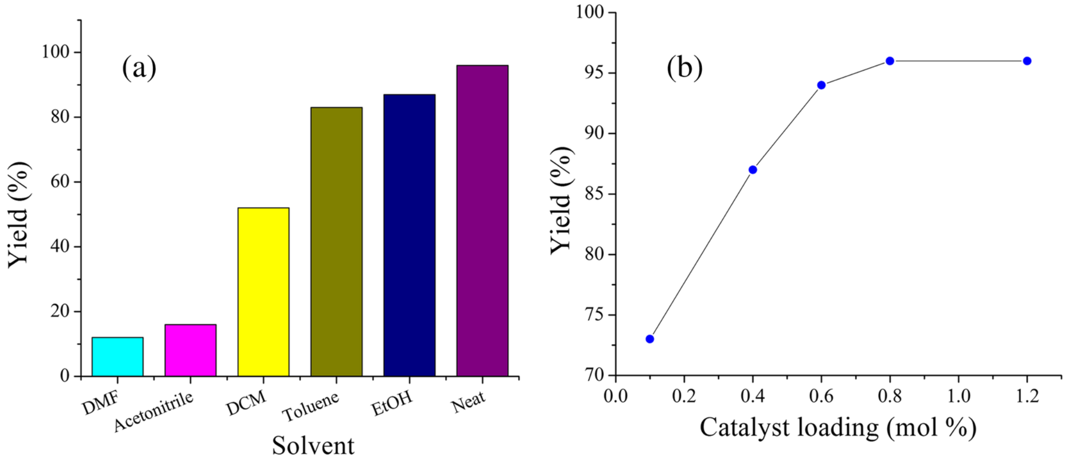

FIGURE 6 (a) Solvent Standardization and (b) Catalyst standardization forcross coupling of acyl chlorides and terminal alkynes

incorporation process of CuO nanoparticles (NPs). The other new diffraction peaks at 2θ = 32.4° (110), 35.3° ($\bar{1}$ 11), 38.05° (111), 48.4° ($\bar{2}$ 02), 53.8° (020), 58.1° (202), 61.3° ($\bar{1}$ 13), 64.4° (311) and 68.1° (220) arises due to CuO nanoparticles.[34] The additional peak observed at 2θ = 44.1° (111) could be because of the presence trace amount of Cu nanoparticles present in the prepared catalyst (Supporting Information, Figure S1).[35]

The TEM image (Figure 3a) of CuO@rGO clearly indicates that the highly monodisperse nature of CuO nanoparticles, having average diameter~5–15 nm have anchored on the surface of rGO. SAED image (Figure 3b) reflects the crystalline nature of CuO@rGO and the EDX spectrum (Figure 3c) reveal the presence of Cu species in CuO@rGO nanocomposites (Supporting Information, Figure S2). The loading of Cu was then estimated by ICP-AES analysis, which shows only 12.8 wt % of Cu exist in the catalyst.

The comparative FT-IR spectrum of GO and CuO@rGO nanocomposites is given in (Figure 4). The FT-IR spectrum of GO shows various characteristic absorption peaks at 3444, 1725, 1396, 1224 and 1046 cm^{-1} corresponding to the hydroxyl (C-OH), carboxyl (O=C-OH), epoxy and alkoxy (C-O) functional groups.[33, 34] The peak at 1622 cm^{-1} corresponds to skeletal vibrations of the graphitic domains.[34] In the

TABLE 2 Screening of the effects of various copper salts as catalyst

Entry	[Cu] catalysts (mol %)	Product	Yield%[aa]
1	$CuCl_2$ (0.8)	3a	trace
2	CuI (0.8)	3a	trace
3	Cu $(OAc)_2$ (0.8)	3a	trace
4	Cu $(NO_3)_2$ (0.8)	3a	trace
5	$CuSO_4$ (0.8)	3a	trace
6	CuBr (0.8)	3a	trace

[a]: Isolated yield of pure product.

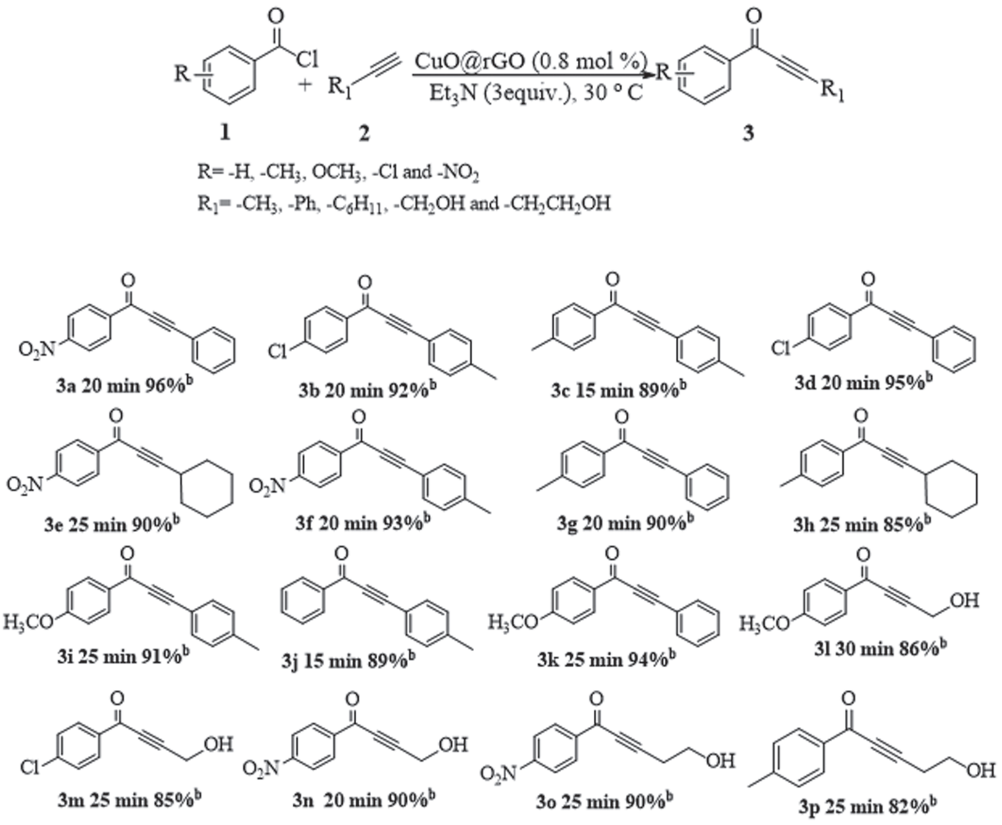

SCHEME 4 Substrate scope for CuO@rGO catalyzed cross coupling of acyl chlorides and terminal alkynes. Reaction conditions: **1** (1.2 nmol), **2** (1 mmol), CuO@rGO (0.8 mol %), Et_3N (3 equiv.), were stirred at 30 °C. [b] Yields of isolated pure products

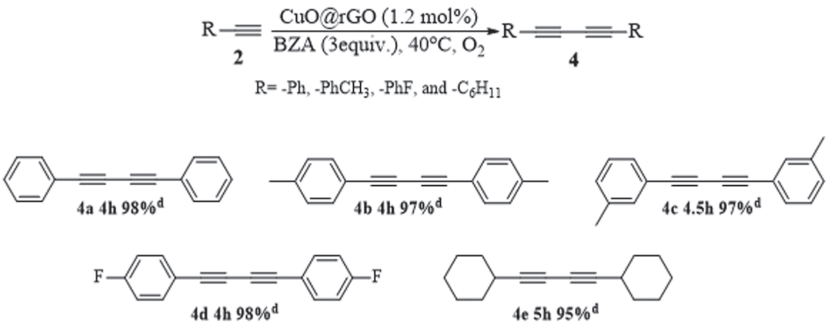

SCHEME 5 Homo-coupling of different terminal alkynes for the synthesis of symmetrical 1,3-diynes. Reaction conditions: **2** (2 nmol), base (3 equiv.), and CuO@rGO (1.2 mol) were allowed to react in a 25 ml round bottom flask under O_2 atmosphere. [d]Yields of isolated pure products

TABLE 3 Screening of reaction conditions for homo-coupling of phenyl acetylene

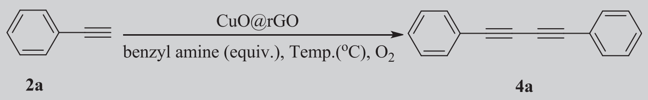

Entry	Catalyst (mol %)	Base	Condition	Temp.(°C)	Time (hr)	Product	Yield (%)[cc]
1	CuO@rGO	Free	air	RT	24	4a	ND
2	Free	BZA(3)	O_2	RT	24	4a	ND
3	CuO@rGO (0.8)	BZA(3)	O_2	50	4	4a	98
4	CuO@rGO (0.8)	BZA(3)	air	40	4	4a	72
5	CuO@rGO (0.8)	BZA(4)	O_2	40	4	4a	98
6	**CuO@rGO (1.2)**	**BZA(3)**	**O_2**	**40**	**4**	**4a**	**98**
7	CuO@rGO (**1.2**)	BZA(3)	O_2	30	4	4a	90
8	CuO@rGO (**1.2**)	DBU	O_2	40	4	4a	ND
9	CuO@rGO (**1.2**)	K_2CO_3	O_2	40	4	4a	ND
10	CuO@rGO (**1.2**)	Cs_2CO_3	O_2	40	4	4a	ND
11	CuO@rGO (**1.2**)	Et_3N	O_2	40	4	4a	12
12	CuO@rGO (**1.2**)	Pyridine	O_2	40	4	4a	32

Reaction conditions: 2a (2 mmol), base (3 equiv.) and CuO@rGO (**1.2 mol %**) were allowed to react in a 25 ml round bottom flask under O_2 atmosphere.

[c]Yields of the pure products. BZA = benzyl amine.

FT-IR spectrum of CuO@rGO, the absorption peaks at 1382 cm^{-1}, 1211 cm^{-1} and 537 cm^{-1} are due to the epoxy and alkoxy and Cu-O stretching vibration respectively.[34] The disappearance of the carboxylic acid peak at 1734 cm^{-1} also indicates the reduction of GO to rGO functionalities (Supporting Information, Figure S3).[36]

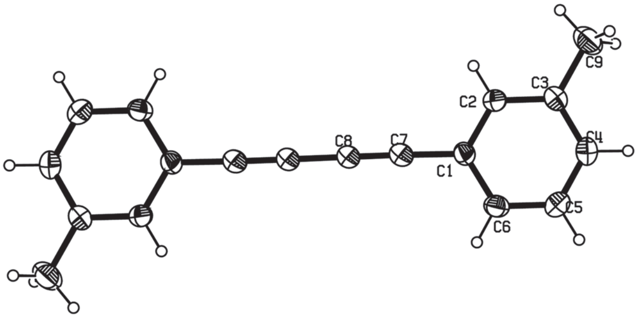

FIGURE 7 Ortep diagram of compound 4c (CCDC 1881184)

The N_2-sorption analysis was performed to investigate the surface area of the CuO@rGO nanocomposites and is shown in Figure 5. The as-synthesized CuO@rGO nanocomposites found to have large BET surface area of about 337 m^2/g respectively (Supporting Information, Figure S4).[34]

After the successful preparation of CuO@rGO, its catalytic activity was investigated for the synthesis of ynones (Scheme 3). Initially, *p*-nitrobenzoyl chloride and phenyl acetylene were chosen as the model substrates. At first, the model reaction was carried out without any catalyst

TABLE 4 Screening of reaction conditions for hetero-coupling of terminal alkynes catalyzed by CuO@rGO

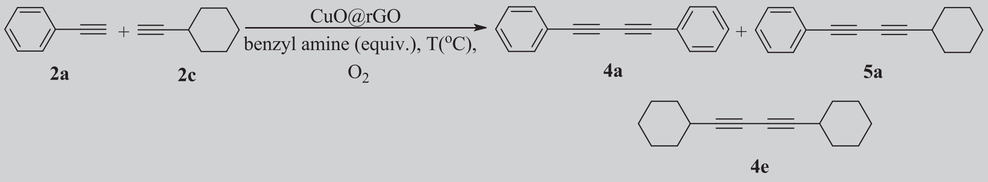

Entry	2a (mmol)	2c (mmol)	Base (equiv.)	4a (yield %)	5a (yield %)	4e (yield %)
1	1	1	BZA(3)	34	45	24
2	1	2	BZA(3)	23	61	32
3	1	3	BZA(3)	12	82	26
4	2	`1	BZA(3)	52	32	18
5	3	1	BZA(3)	67	26	12

in the presence of a base like triethyl amine (Et_3N) and stirred at RT for 24 hr under solvent free reaction condition (SFRC). Reaction failed to produce the desired product and only starting materials were witnessed. Then the reaction was heated at 80 °C for 24 hr. The same result was encountered. Again, when the model reaction was performed in the presence of catalyst CuO@rGO (0.8 mol %, with respect to CuO) at 30 °C, 96% conversion of the product was observed within just 20 min. Further increasing the temperature, the yield remains constant. Therefore, 30 °C is the optimum temperature of this reaction **(**Table 1**)**. It was observed that lowering the catalyst concentration from 0.8 mol % to 0.1 mol %, product yield decreases but higher catalyst loading (0.8 mol %) did not have any effect on product yield (Figure 6b). So, 0.8 mol % is the minimum catalyst concentration for getting the maximum yield.

Next, to check the solvent effect, the model reaction was performed with various solvents like ethanol, toluene, dichloromethane, acetonitrile and dimethylformamide. In EtOH and toluene, the good conversion was achieved but DCM, CH_3CN and DMF showed very poor conversion (Figure 6a). Bases like benzylamine, Cs_2CO_3 and K_2CO_3 performed very inefficiently, furnishing lower yield (Table 1) but triethyl amine afforded the best result. Heteroaromatic bases like pyridine showed inadequacy in producing the desired product (Table 1).

The fate of reaction was then examined with various readily available copper catalysts (0.8 mol %) like CuI_2, $CuCl_2$, Cu $(NO_3)_2$, Cu $(OAc)_{2,}$ $CuSO_4$ and CuBr. They furnished only trace amount of the desired product **3a** (Table 2). After fixing the optimum condition, the generality of the procedure was explored. Variety of acyl chlorides and acetylenes bearing electron donating and electron withdrawing groups were tested, which resulted good to excellent yield of the desired product. It was observed that both aromatic and aliphatic terminal alkynes were well tolerated in this reaction (Scheme 4).

After the successful synthesis of ynones, the catalyst was further utilized for the Glaser oxidative coupling for the preparation of 1,3-diynes. Initially, homo-coupling of phenylacetylene was considered as the model reaction catalyzed by CuO@rGO in presence of

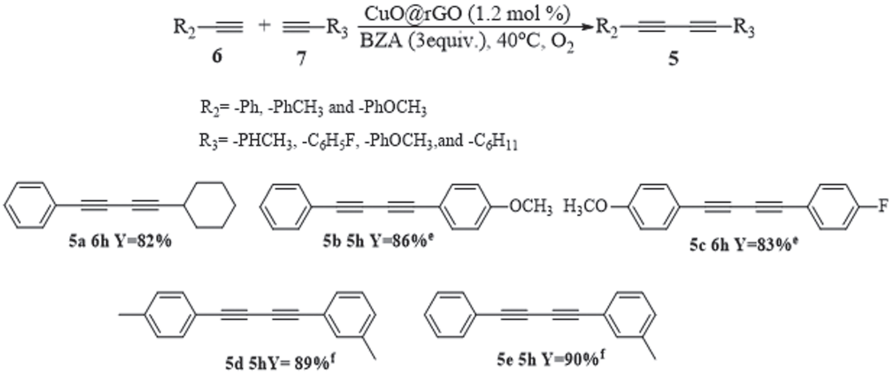

SCHEME 6 Cross-coupling of different terminal alkynes for the synthesis of unsymmetrical 1,3-diynes. Reaction conditions: [e]**6** (2 nmol) and **7** (1 mmol). [f]**6** (1 mmol) and **7** (1 mmol). Y=Isolated yield of pure products

benzylamine as a base under SFRC and O_2 atmosphere. The reaction proceeds well and produced an excellent yield of the homocoupling product **4a**. Then various aromatic terminal alkynes containing both electron-donating and electron withdrawing groups were applied and irrespective of the natures of the substituent, excellent yield (95–98%, Scheme 5) of the desired products (**4a-e**) were obtained. It is clear from Table 3 that the best result was obtained with 1.2 mol % of catalyst. Various other bases such as K_2CO_3, Cs_2CO_3, Et_3N and pyridine were tested (Table 3) but benzyl amine which is cheap and commercially available found to be most efficient in this transformation **4a** (Table 3**, entry 6**). Details screening of the reaction parameters are given in Table 3. Furthermore, the structure of the compound **4c** was confirmed by X-ray crystallography analysis (Supporting Information, Table S1). Figure 7 shows the ortep diagram of compound **4c.**

The catalyst was then successfully utilized for the synthesis of unsymmetrical 1,3-diynes *via* cross-coupling of two different terminal alkynes. First, phenyl acetylene (**2a)** and cyclohexylacetylene (**2c)** were taken as model substrates. The maximum yield 82% of the desired product **5a** was obtained by taking 1:3 molar ratio of **2a** and **2c** **(**Table 4**)**. From the experimental result (Table 4), it can be concluded that alkyne containing electron donating group requires much more molar ratio than electron withdrawing or neutral counterpart. When the reaction was conducted with 4-ethynylanisole and simple phenyl acetylene or 1-ethynyl-4-fluorobenzene, (2:1) molar ratio furnished the excellent yields (86% and 83%) of the final products **5b** and **5c** respectively (Scheme 6).

Due to the huge biological and pharmaceutical application of benzodiazepines, we aimed to synthesize this moiety *via* one pot multicomponent reaction. Along with this line of thinking, benzoylchloride, phenyl acetylene and triethyl amine were reacted in the presence of CuO@rGO at 30 °C for a period of 15–20 min under SFRC. Then *o*-phenylenediamine and ethanol were added to the same vessel and the reaction was continued for at least 2.0–3.0 hr at 60 °C. Various conditions were applied to the model reaction to get the best yield and combination of 0.8 mol % catalyst, triethyl amine (3 equiv.) and EtOH (3 ml) was found to be most efficient to produce the maximum yield of the desired product **6a (**Table 5, **entry 3)**. A little deviation from the standard condition, the lower yield of the expected product **6a** (Table 5) was obtained. After that, various coupling partners like acyl chlorides and terminal acetylenes bearing electron donating and with drawing groups were tested with *o*-phenylenediamines. It was of note that the desired products

TABLE 5 Screening of reaction conditions for the synthesis of 1,5-benzodiazepines

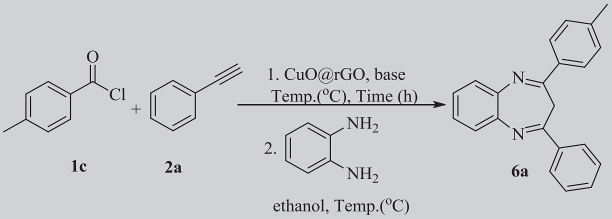

Entry	**Catalyst (mol %)**	**Solvent**	**Temp. (°C)**	**Time (hr)**	**Product**	**Yield (%)**[gg]
1	CuO@rGO (0.8)	Free	RT	24 hr	6a	ND
2	CuO@rGO (0.8)	Free	60	2.20 hr	6a	63
3	**CuO@rGO** (0.8)	**Ehanol**	**60**	**2.20 hr**	**6a**	**82**
4	CuO@rGO (0.8)	Ethanol	70	2.20 hr	6a	82
5	CuO@rGO (0.8)	Ethanol	80	2.20 hr	6a	82
6	CuO@rGO (0.8)	Water	reflux	2.20 hr	6a	56
7	CuO@rGO (0.8)	Dichloromethane	reflux	2.20 hr	6a	27
8	CuO@rGO (0.8)	Acetonitrile	reflux	2.20 hr	6a	12
9	CuO@rGO (0.8)	Dimethylformamide	reflux	2.20 hr	6a	ND

Reaction conditions: Reactions were carried out using **1c** (1.2 mmol), **2a** (1 mmol), diamine (1.3 mmol), 0.8 mol % of catalyst, CuO@rGO and ethanol (3 ml).

[g] Yield of isolated pure products.

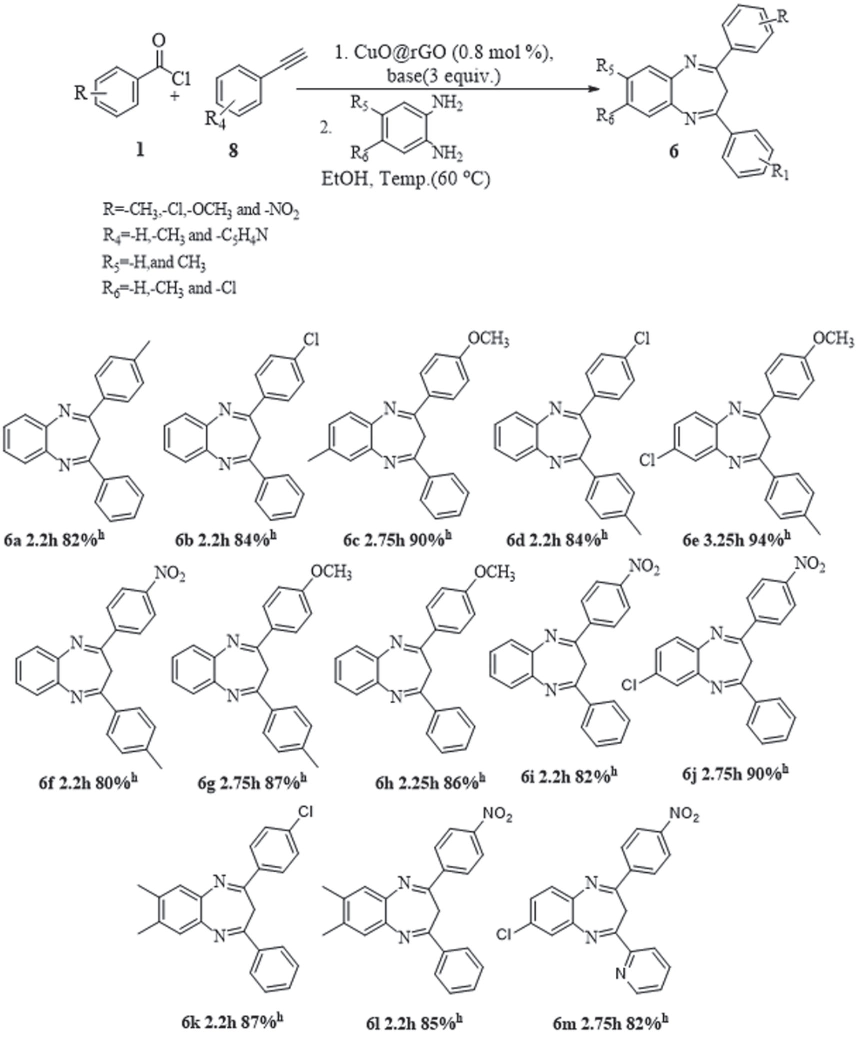

SCHEME 7 Substrate scope for the preparation of 1,5-benzodiazepines catalyzed by CuO@rGO. Reaction conditions: **1** (1.2 mmol), **8** (mmol) diamine (1.3 mmol), were stirred at 60 °C in presence of 0.8 mol % of catalyst, CuO@rGO and EtOH (3 ml). [h] Yieids of isolated pure products

were obtained in good to excellent yield and functional groups have no effect on the yield of the products (Scheme 7). The structure of the compound **6a** was further confirmed by X-ray crystallography (Supporting Information, Table S1). Figure 8 shows the ortep diagram of compound **6a**.

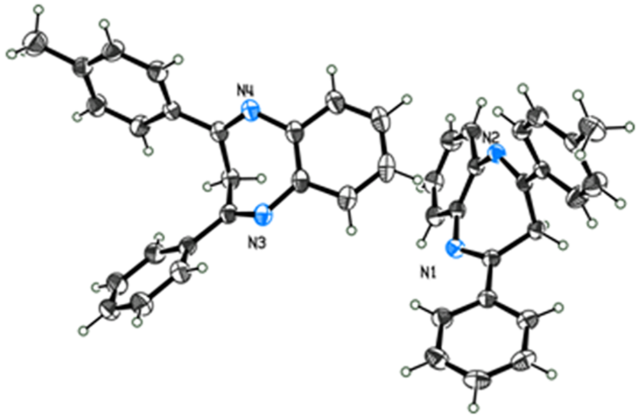

FIGURE 8 Ortep diagram of compound 6a (CCDC 1916396)

The leaching test was carried out for the cross coupling of acyl chloride and phenylacetylene (Scheme 3). The reaction was initially stirred for 10 min. After that, the reaction mixture was dissolved in chloroform and the catalyst was removed by filtration. The solvent was then removed from the reaction mixture and the residue was stirred again for another 20 min under the same reaction condition. It was observed that after removing the catalyst product yield was not increased, which in turn proved that there was no or very negligible leaching of the catalyst.

The reusability of heterogeneous catalysts plays a key role in its practical application in many organic transformations over the homogeneous catalysts. Therefore, the performance of the recovered catalyst was investigated and it was observed that the activity of recovered CuO@rGO remains almost unchanged up to seventh consecutive runs. The histogram chart of the reused catalyst showing the corresponding yield of the reaction up to seven consecutive runs is shown in Figure 9.

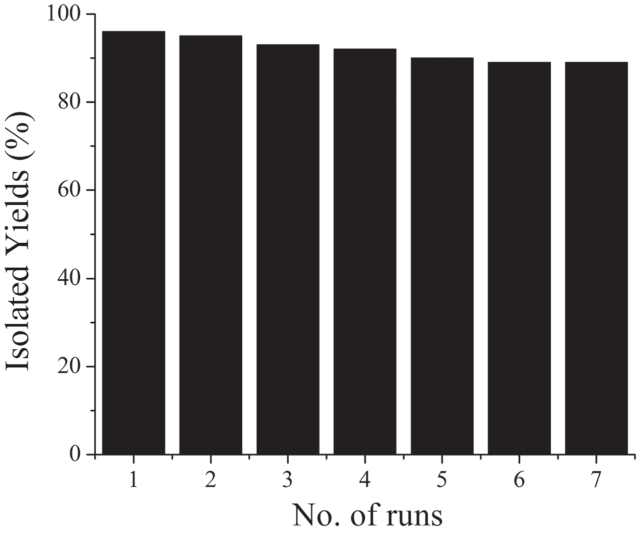

FIGURE 9 Reusability of CuO@rGO nanocomposites up to seven runs

3 | CONCLUSION

In conclusion, we have developed new avenues for the synthesis of ynones, 1,3-diynes and 1,5-benzodiazepines catalyzed by a single, efficient and reusable CuO@rGO catalyst. Notably, good to excellent yield of the desired products, a short interval of time and reusability are the advantages of the protocols. Furthermore, the experimental results demonstrate that the CuO nanoparticles are well distributed over the rGO sheets owing to its higher catalytic activity and recyclability. Solvent free reaction conditions, low catalyst loading and reusability of catalyst satisfy some of the green chemistry principles.

ACKNOWLEDGMENTS

We thank Science and Engineering Research Board (SERB, EMR/2016/005089 dated 30.6.2017), Department of Chemistry of North-Eastern Hill University (NEHU) and University Grant Commission We are grateful to Sophisticated Analytical and Instrumentation Facility (SAIF) and Department of nanotechnology of North-Eastern Hill University and Department of CSS,Indian Association of Cultivation of Science (IACS), Kolkata. We also take this opportunity to thank Dr. Snehadrinarayan Khatua, Department of Chemistry, North-Eastern Hill University, Shillong.

ORCID

Rajib Sarkar https://orcid.org/0000-0001-7838-3804

REFERENCES

[1] A. V. Kel, V. Gevorgyan, *J. Org. Chem.* **2002**, *67*, 95.
[2] L. Wang, G. Li, Y. Liu, *Org. Lett.* **2011**, *13*, 3786.
[3] M. W. Logue, G. L. Moore, *J. Org. Chem.* **1975**, *40*, 131.
[4] J. W. Nieuwland, J. A. Kroeger, *J. Am. Chem. Soc.* **1936**, *58*, 1861.
[5] R. B. Davis, D. H. Scheiber, *J. Am. Chem. Soc.* **1956**, *78*, 1675.
[6] Y. Nishihara, D. Saito, E. Inoue, Y. Okada, M. Miyazaki, Y. Inoue, Y. Takagi, *Tetrahedron Lett.* **2010**, *51*, 306.
[7] D. R. Waiton, F. J. Waugh, *Organomet. Chem.* **1972**, *37*, 45.
[8] I. E. Marko, J. M. Southern, *J. Org. Chem.* **1990**, *55*, 3368.
[9] Y. Han, L. Fang, W. T. Tao, Y. Z. Huang, *Tetrahedron Lett.* **1995**, *36*, 1287.
[10] N. Kakusawa, K. Yamaguchi, J. Kurita, T. Tsuchiya, *Tetrahedron Lett.* **2000**, *41*, 4143.
[11] I. Perez, J. P. Sestelo, L. A. Sarandeses, *J. Am. Chem. Soc.* **2001**, *123*, 4155.
[12] K. Y. Lee, M. J. Lee, J. N. Kim, *Tetrahedron* **2005**, *61*, 8705.
[13] C. Zhang, J. Liu, C. Xia, *Org. Biomol. Chem.* **2014**, *12*, 9702.
[14] M. Cui, H. Wu, J. Jian, H. Wang, C. Liu, S. Daniel, *Chem. Commun.* **2016**, *52*, 12076.
[15] E. Mohammadi, B. Movassag, M. Navidi, *Helv. Chim. Acta* **2014**, *97*, 70.
[16] R. E. Islas, J. Cardenas, R. Gavino, E. Garcia-Rios, L. Lomas-Romero, J. A. Morales-Serna, *RSC Adv.* **2017**, *7*, 9780.
[17] L. Chen, C. J. Li, *Org. Lett.* **2004**, *6*, 3151.
[18] R. Chutia, B. Chetia, *Tetrahedron Lett.* **2017**, *58*, 3864.
[19] I. J. S. Fairlamb, P. S. Bauerlein, L. R. Marrison, J. M. Dickinson, *Chem. Commun.* **2003**, 632.
[20] H. Xu, K. Wu, J. Tian, L. Zhu, X. Yao, *Green Chem.* **2018**, *20*, 793.
[21] S. Biswas, K. Mullick, Y. S. Chen, D. A. Kriz, M. D. Shakil, C. H. Kuo, A. M. Angeles-Boza, A. R. Rossi, S. L. Suib, *ACS Catal.* **2016**, *6*, 5069.
[22] M. Pan, J. Gong, G. Dong, C. B. Mullins, *Acc. Chem. Res.* **2014**, *47*, 750.
[23] M. Imran, A. B. Yousaf, X. Zhou, Y.-F. Jiang, C.-Z. Yuan, A. Zeb, N. Jiang, A.-W. Xu, *J. Phys. Chem. C* **2017**, *121*, 1162.
[24] A. Biffis, P. Centomo, A. D. Zotto, M. Zecca, *Chem. Rev.* **2018**, *118*, 2249.
[25] R. J. White, R. Luque, V. L. Budarin, J. H. Clark, D. J. Macquarrie, *Chem. Rev.* **2009**, *38*, 481.
[26] Y. Choi, H. S. Bae, E. Seo, S. Jang, K. H. Park, B. S. Kim, *J. Mater. Chem.* **2011**, *21*, 15431.
[27] B. Willy, T. Dallos, F. Rominger, J. Schonhaber, T. J. J. Muller, *Eur. J. Org. Chem.* **2008**, 4796.
[28] A. Solan, B. Nisanci, M. Belcher, A. Young, C. Schafer, K. A. Wheeler, B. Torok, R. Dembenski, *Green Chem.* **2014**, *16*, 1120.
[29] S. G. Huang, H. F. Mao, S. F. Zhou, J. P. Zou, W. Zhang, *Tetrahedron Lett.* **2013**, *54*, 6178.
[30] S. S. Palimkar, R. J. Lahoti, K. V. Srinivasan, *Green Chem.* **2007**, *9*, 146.
[31] W. S. Hummers Jr., R. E. Offeman, *J. Am. Chem. Soc.* **1958**, *80*, 1339.
[32] A. Gupta, R. Jamatia, R. A. Patil, Y.-R. Ma, A. K. Pal, *ACS Omega* **2018**, *3*, 7288.
[33] R. Jamatia, A. B. Dam, M. Saha, A. K. Pal, *Green Chem.* **2017**, *19*, 1576.
[34] Y. Zhao, X. Song, Q. Song, Z. Yin, *CrystEngComm* **2012**, *14*, 6710.

[35] M. S. Usman, N. A. Ibrahim, K. Shameli, N. Zainuddin, W. M. Z. W. Yunus, *Molecules* **2012**, *17*, 14928.

[36] A. M. Jastrzebska, J. Karcz, R. Letmanowski, D. Zabost, E. Ciecierska, M. Siekierski, A. Olszyna, J. Alloys, *Compd.* **2016**, *679*, 470.

SUPPORTING INFORMATION

Additional supporting information may be found online in the Supporting Information section at the end of this article.

How to cite this article: Sarkar R, Gupta A, Jamatia R, Pal AK. Reduced graphene oxide supported copper oxide nanocomposites: An efficient heterogeneous and reusable catalyst for the synthesis of ynones, 1,3-diynes and 1,5-benzodiazepines in one-pot under sustainable reaction conditions. *Appl Organometal Chem*. 2020; e5646. https://doi.org/10.1002/aoc.5646